Modeling & Numerical Simulation of Hypersonic Flows

Thierry Magin

BRussels Institute for Thermal-fluid systems and clean Energy (BRITE)
Aero-Thermo-Mechanics (ATM), Université Libre de Bruxelles, Belgium

Aeronautics and Aerospace Department
von Karman Institute for Fluid Dynamics, Belgium

ERCOFTAC Autumn Festival 2023

12 – 13 October 2023, Liège, Belgium

Developing disruptive technology for hypersonics

- Hypersonics
  - Fight within planetary atmosphere at Mach > 5

- Challenges for fluid models and numerical methods
  - Multiscale and multiphysics problem
  - Calibration and validation of computational models

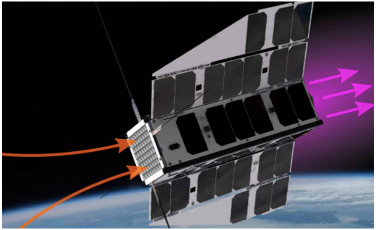

Air Breathing Electric Propulsion concept
for Very Low Earth Orbit observation

Orion Crew Module reentry
14 November 2022 (Artemis I)

“Aerothermochemistry” coined by von Kármán

> *“With the advent of jet propulsion, it became necessary to broaden the field of aerodynamics to include problems which before were treated mostly by physical chemists...”* Theodore von Kármán, 1958

- Some open problems
  - Fluid models for thermo-chemical nonequilibrium
  - High-order methods for hypersonic flows
  - Efficient solvers for 3D plasma sheath

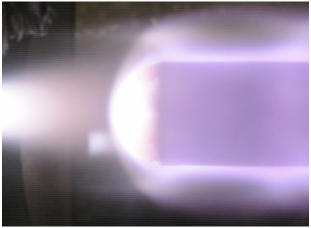

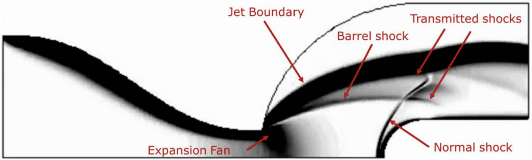

[Capriati, Turchi, Congedo, M., 9th EUCASS 2022]

Under-expanded air jet over catalytic probe in VKI Plasmatron

Fluid models beyond Navier-Stokes. . .

- Kinetic theory allows us to
  - Describe plasmas in the rarefied regime
  - Derive asymptotic fluid solutions

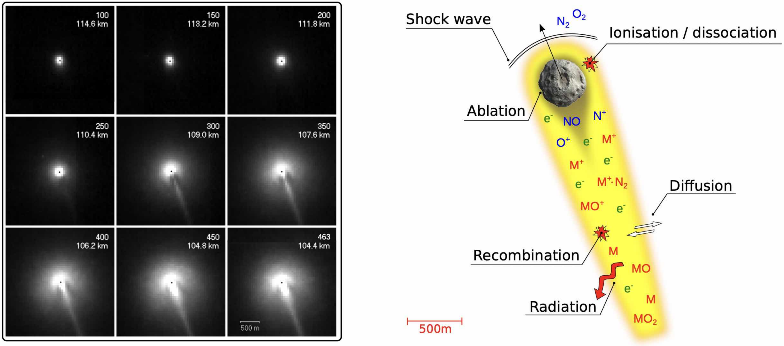

[Bariselli, Boccelli, Dias, Hubin, M., Astronomy & Astrophysics 2020]

Meteors can be detected by scattering of electromagnetic waves by electrons in rarefied trail

MUlticomponent Thermodynamic And Transport properties for IONized gases library written in C++

Mutation++

Multicomponent Thermodynamic And Transport properties for IONized gases in C++

https://github.com/mutationpp/Mutationpp

[Scoggins, Leroy, Bellas-Chatzigeorgis, Dias, M., Software X 2017]

- Centralizes physico-chemical models, algorithms, and data for reactive and plasma flows into a single software package
- Can be shared among CFD tools

Outline

Coarse-grain transport models consistent from the kinetic to fluid regimes

Simulation of plasma sheath

Atmospheric entry simulation

Calibration of models

Microscopic approach to derive macroscopic nonequilibrium models...

- Developing high-fidelity models physics-based
- NASA ARC database for nitrogen chemistry
    - 9390 (v,J) rovibrational energy levels for $\mathrm{N_2}$
    - 50×10^6 reaction mechanism for $\mathbf{N_2} + \mathbf{N}$ system

$$\mathrm{N_2(v, J) + N \leftrightarrow N + N + N}$$

$$\mathrm{N_2(v, J) + N \leftrightarrow N_2(v', J') + N}$$

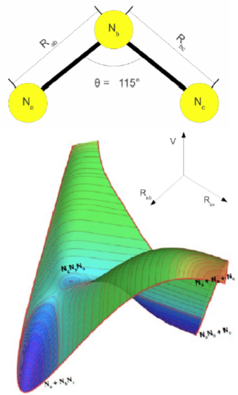

$\mathrm{N_3}$ Potential Energy Surface

NASA Ames Research Center

Kinetic equation for coarse-grain model

[Torres, Bellas-Chatzigeorgis, M., Physics of Fluids, 2021]

- Set of species

$$\mathcal{S} = \{\mathrm{N}, \mathrm{N}_2\,(k)\,|\,(k = 1, 2, \dots, n_{\mathrm{bins}})\}$$

- Boltzmann equation (1D space 3D velocity)

$$\frac{\partial f_{\mathrm{N}}}{\partial t} + c_x\,\frac{\partial f_{\mathrm{N}}}{\partial x} = \frac{1}{\varepsilon}\mathcal{J}\,(f_{\mathrm{N}}, f_{\mathrm{N}}) + \frac{1}{\varepsilon}\sum_{l\in\mathcal{K}_{\mathrm{N}_2}} \mathcal{J}\,(f_{\mathrm{N}}, f_l) + \varepsilon\;\mathcal{C}_{\mathrm{N}}$$

$$\frac{\partial f_k}{\partial t} + c_x\,\frac{\partial f_k}{\partial x} = \frac{1}{\varepsilon}\mathcal{J}\,(f_k, f_{\mathrm{N}}) + \frac{1}{\varepsilon}\sum_{l\in\mathcal{K}_{\mathrm{N}_2}} \mathcal{J}\,(f_k, f_l) + \varepsilon\;\mathcal{C}_k, \quad k \in \mathcal{K}_{\mathrm{N}_2}$$

  - Reactive collisions are assumed to follow the Maxwellian regime
  - Consistency between the kinetic and fluid regimes is a direct consequence of the asymptotic analysis of the Boltzmann eq.

Fluid regime: Navier-Stokes eqs.

- Enskog expansion

$$f_i = f_i^0(1 + \varepsilon\phi_i), \quad i \in \mathcal{S}$$

- Chapman-Enskog perturbative solution method yields

$$\frac{\partial \rho_{\mathrm{N}}}{\partial t} + \frac{\partial}{\partial x}\left(\rho_{\mathrm{N}}\, u + \rho_{\mathrm{N}}\, u_{\mathrm{N}}^{\mathrm{d}}\right) = \omega_{\mathrm{N}}$$

$$\frac{\partial \bar{\rho}_k}{\partial t} + \frac{\partial}{\partial x}\left(\bar{\rho}_k\, u + \bar{\rho}_k\, \bar{u}_k^{\mathrm{d}}\right) = \bar{\omega}_k, \qquad k \in \mathcal{K}_{\mathrm{N}_2}$$

$$\frac{\partial \rho u}{\partial t} + \frac{\partial}{\partial x}\left(\rho u^2 + p - \tau_{xx}\right) = 0$$

$$\frac{\partial \rho E}{\partial t} + \frac{\partial}{\partial x}\left(\rho u\left(E + \frac{p}{\rho}\right) - \tau_{xx}\, u + q_x\right) = 0$$

- Chemical production rates satisfy the law of mass action
- The forward and backward rate coefficients are linked to an equilibrium constant consistent with the system thermodynamics

Entropy eq. (2nd law of thermodynamics)

$$\frac{\partial(\rho s)}{\partial t}+\frac{\partial}{\partial x}(\rho s\, u)+\frac{\partial}{\partial x}J_S=\Upsilon$$

- Entropy flux

$$J_S=\frac{q}{T}-\sum_{k\in\mathcal{K}_{\mathrm{N}_2}}\bar{\rho}_k\,\bar{u}_k^{\mathrm{d}}\,\frac{\bar{g}_k}{T}-\rho_{\mathrm{N}}\,u_{\mathrm{N}}^{\mathrm{d}}\,\frac{g_{\mathrm{N}}}{T}$$

- Entropy production

$$\Upsilon\geq 0$$

  - First coarse-grain model equipped with a transport theory that satisfies the laws of thermodynamics

Viscous (Navier-Stokes) versus inviscid (Euler) solution (shock wave, u = 10 km/s)

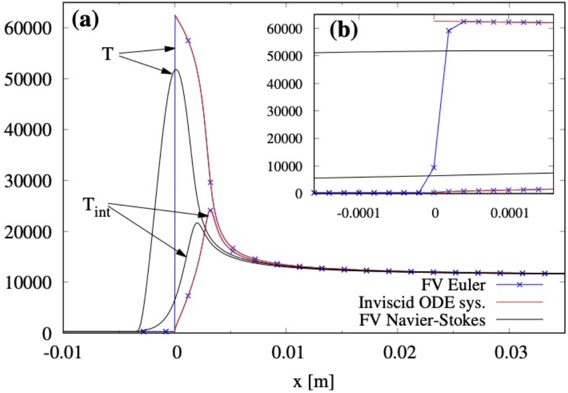

- Euler FV solutions not polluted by numerical diffusion
- Any diffusive effects observed in the Navier–Stokes profiles are physical in nature, i.e., exclusively due to the actual molecular diffusion terms

Viscous (Navier-Stokes) versus DSMC solution (shock wave, u = 10 km/s)

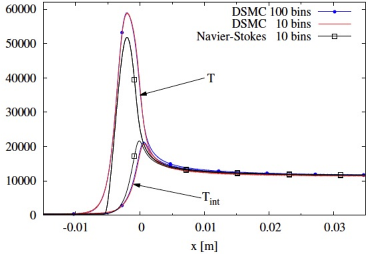

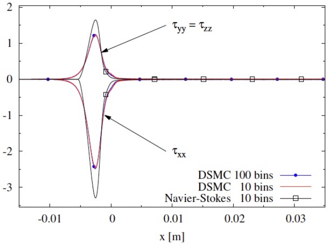

- For these flight conditions, good agreement found between kinetic (DSMC) and fluid (CFD) solutions
- Consistency of the cross-sections / rate coefficients is crucial

Outline

Coarse-grain transport models consistent from the kinetic to fluid regimes

Simulation of plasma sheath

Atmospheric entry simulation

Calibration of models

Plasma-wall interaction: sheath

- Sheath
  - Layer in a plasma which has a greater density of positive ions

- Challenges
  - Sheath thickness becomes small as pressure increases
  - Multifluid models become expensive as number of species increases

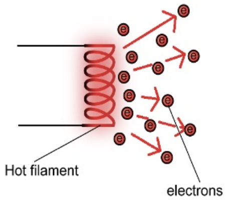

Thermionic emission used in electron transpiration cooling

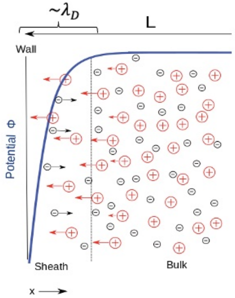

Plasma sheath

Dimensional analysis for plasmas [Petit, Darrozes 1975]

- 2 kinetic temporal scales based on common mean-free-path l^0

$$t_{\mathrm{e}}^0 = \frac{l^0}{V_{\mathrm{e}}^0}, \qquad t_h^0 = \frac{l^0}{V_h^0} = \frac{1}{\varepsilon} t_{\mathrm{e}}^0 \quad \text{with} \quad \varepsilon = \frac{V_h^0}{V_{\mathrm{e}}^0} = \sqrt{\frac{m_{\mathrm{e}}}{m_h}}$$

- 1 macroscopic temporal scale based on macroscopic length L^0

$$t^0 = \frac{L^0}{V_h^0} = \frac{1}{Kn} t_h^0 \quad \text{with} \quad Kn = \frac{l^0}{L^0}$$

Nondimensional form and scaling of Boltzmann eq.

- Electrons: e

$$\partial_t f_{\mathrm{e}} + \frac{1}{\varepsilon}\boldsymbol{c}_{\mathrm{e}}\cdot\boldsymbol{\partial}_{\boldsymbol{x}} f_{\mathrm{e}} + \frac{1}{\varepsilon} q_e \boldsymbol{E}\cdot\boldsymbol{\partial}_{\boldsymbol{c}_{\mathrm{e}}} f_{\mathrm{e}} = \frac{1}{\varepsilon Kn}\Big[\mathcal{J}_{\mathrm{ee}}(f_{\mathrm{e}}, f_{\mathrm{e}}) + \sum_{j\in\mathrm{H}} \mathcal{J}_{\mathrm{e}j}(f_{\mathrm{e}}, f_j)\Big]$$

- Heavy particles: $i \in \mathrm{H}$

$$\partial_t f_i + \boldsymbol{c}_i\cdot\boldsymbol{\partial}_{\boldsymbol{x}} f_i + \tfrac{q_i}{m_i}\boldsymbol{E}\cdot\boldsymbol{\partial}_{\boldsymbol{c}_i} f_i = \frac{1}{Kn}\Big[\frac{1}{\varepsilon}\mathcal{J}_{i\mathrm{e}}(f_i, f_{\mathrm{e}}) + \sum_{j\in\mathrm{H}} \mathcal{J}_{ij}(f_i, f_j)\Big]$$

- Multiscale assympotic analysis with entangled parabolic and hyperbolic scalings [Graille, M., Massot 2009]

$$\varepsilon = Kn$$

  - **Electrons**: low Mach number regime
    [Bardos, Golse, Levermore, 1991]
  - **Heavy particles**: compressible gas dynamics regime
    [Goudon, Jabin, Vasseur, 2005]

Multifluid scaling of Boltzmann eq.

- Kinetic equation for species $i \in \mathrm{S}$

$$\partial_t f_i + \boldsymbol{c}_i \cdot \boldsymbol{\partial}_{\boldsymbol{x}} f_i + \frac{\boldsymbol{F}_i}{m_i} \cdot \boldsymbol{\partial}_{\boldsymbol{c}_i} f_i = \sum_{j \neq i} \mathcal{J}_{ij}(f_i, f_j) + \frac{1}{\varepsilon} \mathcal{J}_{ii}(f_i, f_i) + C_i^r$$

  - Fluid equations are decoupled for each species
  - Example: isothermal ion - electron mixture in neutral bath

$$\begin{aligned}
\partial_t n_e + \partial_x (n_e u_e) &= n_e \nu^{iz} \\
\partial_t n_i + \partial_x (n_i u_i) &= n_e \nu^{iz} \\
\partial_t (n_e u_e) + \partial_x \left(n_e u_e^2 + \frac{p_e}{m_e} \right) &= \frac{n_e e}{m_e} \partial_x \phi - n_e u_e \nu_{en} \\
\partial_t (n_i u_i) + \partial_x \left(n_i u_i^2 + \frac{p_i}{m_i} \right) &= -\frac{n_i e}{m_i} \partial_x \phi - n_i u_i \nu_{in}
\end{aligned}$$

- Coupling to Poisson's eq.

$$\partial_{xx}^2 \phi = \frac{e (n_e - n_i)}{\varepsilon_0}$$

Comparison multifluid / multicomponent diffusion models

- Binary diffusion model

$$\begin{aligned} \partial_t n_e + \partial_x (n_e V_e) &= n_e \nu^{iz} \\ \partial_t n_i + \partial_x (n_i V_i) &= n_e \nu^{iz} \end{aligned}$$

  - Diffusion velocity: $V_k = -\frac{D_k}{n_k}\partial_x n_k - \mu_k \partial_x \phi$
  - Binary diffusion coefficient: $D_k = \frac{k_B T_k}{m_k \nu_{kn}}$
  - Species mobility: $\mu_k = \frac{q_k}{m_k \nu_{kn}}$

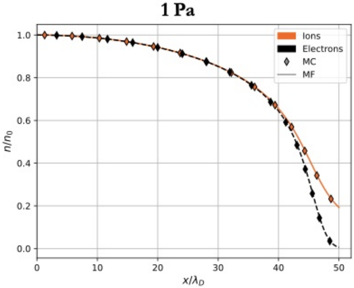

Simulation of 1D plasma sheath at 1 Pa between 2 walls

[Gangemi, Alvarez Laguna, Hillewaert, M., 9th EUCASS 2022]

Air-Breathing Electric Propulsion (ABEP)

- Residual atmosphere drag compensated by thrust
- ABEP systems collect atmospheric molecules through intake
- Air propellant for electric thruster, no lifetime limitation!

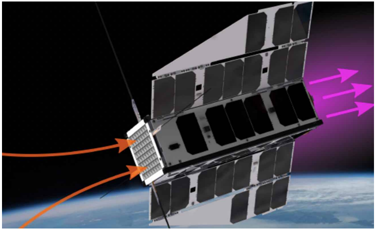

Air Breathing Electric Propulsion concept
for Very Low Earth Orbit observation

VKI DRAGON low-density facility

PIC/DSMC plasma simulation (PANTERA code)

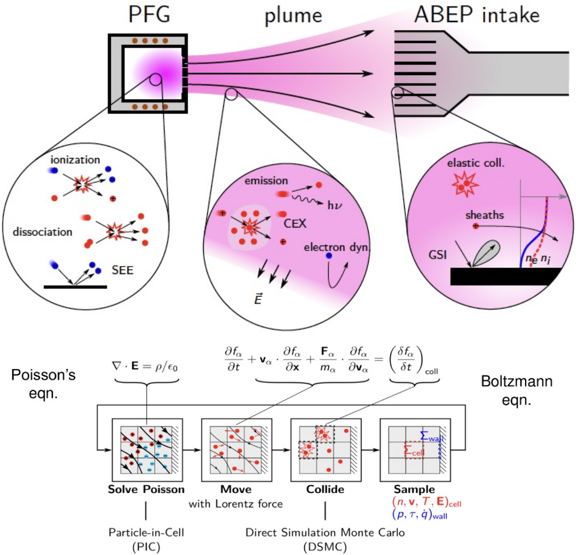

[Parodi, Lapenta, M., GEC 2022]

Plasma plume simulation with semi-implicit scheme

- Plasmas of our interest span multiple length- and time scales
- With an explicit PIC scheme no choice but to resolve these
- Fully-implicit methodology with Jacobian computed from the actual particle motion in the grid

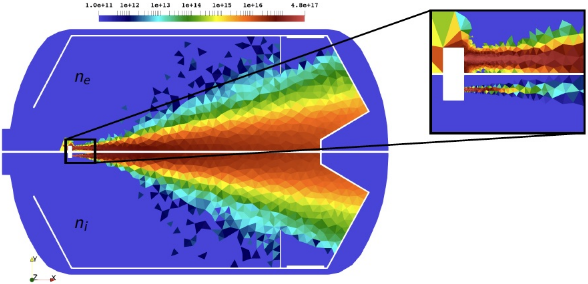

[Parodi, Lapenta, M., GEC 2022]

Outline

Coarse-grain transport models consistent from the kinetic to fluid regimes

Simulation of plasma sheath

Atmospheric entry simulation

Calibration of models

Development of integrated codes for flow /radiation/ material coupling

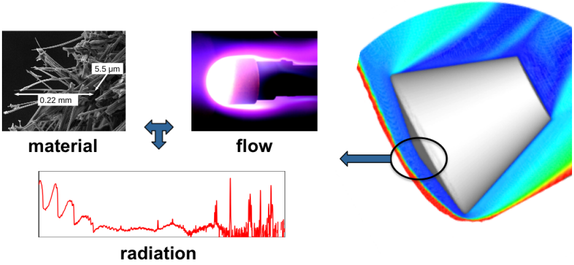

- Ablative material / flow coupling

  Pyrolysis gas blows in the boundary layer
- Flow / radiation coupling

  Radiation field depends on flow excited species concentration
- Ablative material / radiation coupling

  Ablation products can absorb the shock layer radiation

Apollo 4 peak heating trajectory point

- First flight of Saturn V rocket and all-up test of Apollo systems (unmanned)
- Ablative TPS
- Radiometer aligned at stagnation point
- Fore body was a 33¡ sphere segment with nose radius of 4.69 m
- Equivalent sphere radius of 2.85 m to reproduce shock standoff distance [Park, 2004]

Time s	Altitude km	V_∞ km/s	ρ_∞ kg/m^3	T_∞ K
30020	67.47	10.640	$1.13\cdot 10^{-4}$	224.53
30024	64.55	10.511	$1.73\cdot 10^{-4}$	232.71
30028	61.99	10.382	$2.50\cdot 10^{-4}$	239.88
30032	59.79	10.252	$3.41\cdot 10^{-4}$	246.04
30036	58.00	10.042	$4.31\cdot 10^{-4}$	251.05
30040	56.69	9.798	$5.01\cdot 10^{-4}$	254.72
30044	55.89	9.534	$5.51\cdot 10^{-4}$	256.96

Simulation of Apollo 4 peak heating trajectory point

Coupling strategy	$\epsilon(\sigma T^4 + q_w^{rad})$ W/cm^2	ϵq_w^{rad} W/cm^2	q_w^{diff} W/cm^2	q_w^{cond} W/cm^2	q_w^{conv} W/cm^2	$\dot{m}(h_w - h_s)$ W/cm^2
Flow	−91.64	−279.92	−2.70	−119.77	−122.47	-
Flow / Abl.	−66.46	−254.74	−38.62	−95.31	−133.93	5.99
Flow / Rad.	−8.36	−196.64	−4.56	−168.42	−172.98	-
Fully Coupled	−6.16	−194.44	−37.77	−97.38	−135.15	5.79

[Scoggins, PhD thesis 2017]

- Shock layer radiative cooling due to strong plasma emission
- Ablation products released by the heat shield contribute to increased radiation blockage in the boundary layer

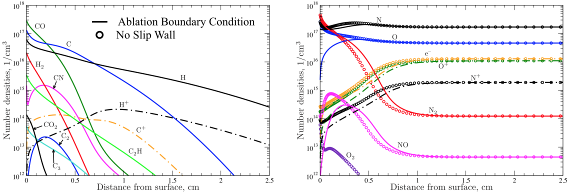

⇒ Strong coupling between the flow / radiation / material fields

Comparison to radiometer flight data

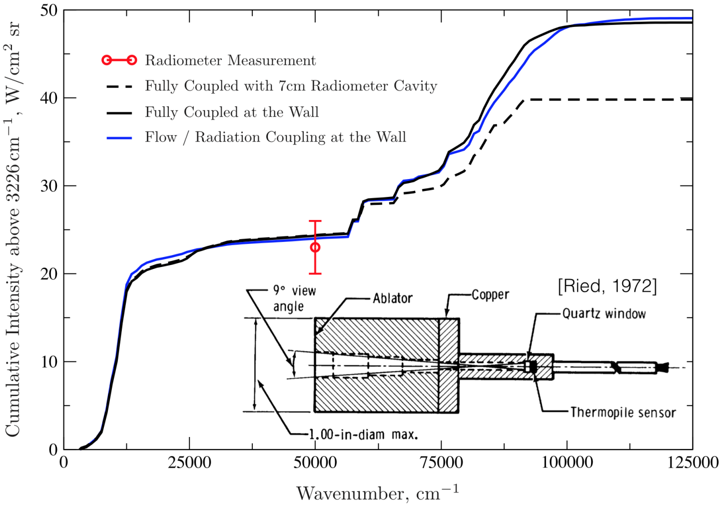

[Ried, 1972]

Development of a unified solver to treat reactive porous material and high enthalpy flows

- Implementation in the Argo code (CENAERO)
  [Schrooyen, Dias, Fagnani, Turchi, Helber, Walpot, M., FAR 2022]

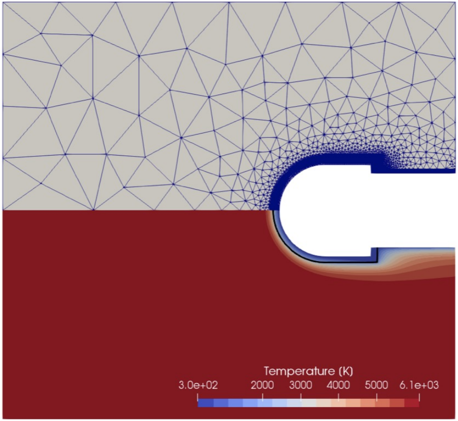

Mass :

- *Gas*

$$\frac{\partial \epsilon_g \langle \rho_i \rangle_g}{\partial t} + \nabla \cdot (\epsilon_g \langle \rho_i \rangle_g \langle u \rangle_g) = \nabla \cdot \left(\epsilon_g \frac{D_{i,m}}{\eta} \langle \rho_i \rangle_g \frac{W_i}{W} \nabla X_i \right) + \langle \dot{\omega} \rangle + \Pi_g$$

- *Solid (fibers + char + resin)*

$$\frac{\partial \epsilon_s \langle \rho_s \rangle_s}{\partial t} = \langle \dot{\omega}^{het} \rangle - \Pi_g$$

Momentum :

$$\frac{\partial (\epsilon_g \langle \rho u \rangle_g)}{\partial t} + \nabla \cdot (\epsilon_g \langle \rho \rangle_g \langle u \rangle_g \langle u \rangle_g) = -\epsilon_g \nabla \langle P \rangle_g + \nabla \cdot \langle \tau \rangle + F$$

Energy :

$$\frac{\partial \langle \rho E_{tot} \rangle}{\partial t} + \nabla \cdot (\epsilon_g \langle \rho \rangle_g \langle H \rangle_g \langle u \rangle_g) = \nabla \cdot (\lambda_{eff} \nabla T) + \nabla \cdot (\langle \tau \cdot u \rangle)$$

Outline

Coarse-grain transport models consistent from the kinetic to fluid regimes

Simulation of plasma sheath

Atmospheric entry simulation

Calibration of models

US3D CFD solver for hypersonic flows (U Minnessota)

- 3D Finite-Volume discretization
- Modified Steger-Warming numerical scheme with MUSCL reconstruction
- Data Parallel Line Relaxation (DPLR) to obtain rapid convergence to steady-state

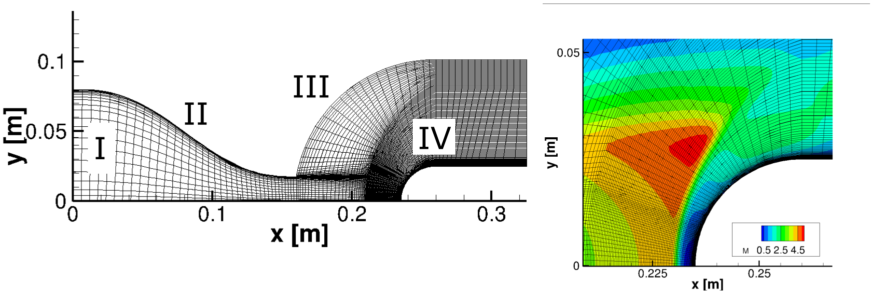

Left: computational domain I) exit of plasma torch, II) sonic nozzle surface, III) expansion chamber and IV) probe. **Right**: zoom on numerical grid adapted with the shock to avoid carbuncle
[Capriati, Turchi, Congedo, M., 9th EUCASS 2022]

Multifidelity surrogate model based on hierarchical Kriging

Tag	cells	Δx [m]	h_i	t_{CPU} [min]
I	172224	5E-7	1	$\approx$ 1600
II	43056	1E-6	2	$\approx$ 200
III	10764	2E-6	4	$\approx$ 30
IV	2691	4E-6	8	$\approx$ 4

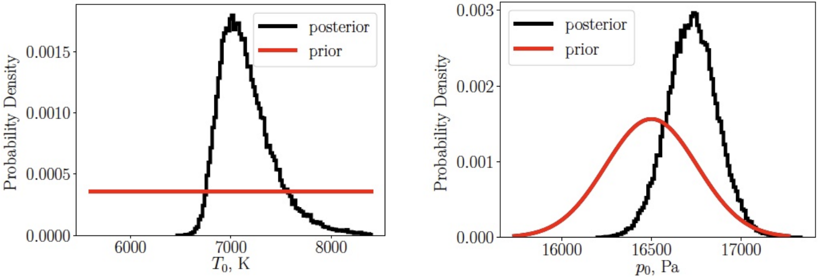

Prior and posterior marginal distributions for the QoIs.

[Capriati, Turchi, Congedo, M., 9th EUCASS 2022]

Stochastic calibration of carbon nitridation model from plasma wind tunnel experiments

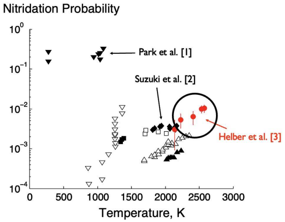

Bayesian inference

methodology

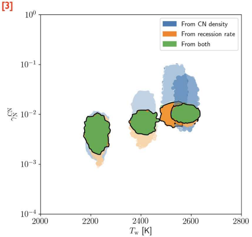

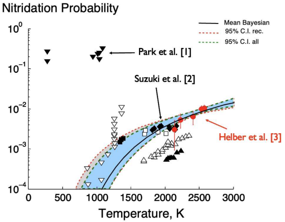

Integration of all available

measurements from Helber *et al.*

$$\gamma_N^{CN} = A\exp\left(\frac{-T_a}{T_w}\right)$$

[del Val, Lemaitre, Congedo, M., Carbon 2022]

Conclusion

- Hypersonics is a multiscale and multiphysics problem
- Kinetic theory is a powerful tool to derive sound fluid models for plasmas
- Well identified mathematical structure of the conservation eqs. allows for development of numerical schemes
- Don't forget to calibrate and validate your computational models!

Thank you!

- Collaborators who contributed to the results presented
  - Koen Hillewaert (U Liège)
  - Philippe Chatelain (UC Louvain)
  - Giovanni Lapenta (KULeuven)
  - Nagi Mansour (NASA Ames)
  - Alejandro Alvarez Laguna, Anne Bourdon, Pietro Congedo, Vincent Giovangigli, Olivier Lemaitre, Marc Massot, (Ecole Polytechnique)
  - **VKI**: George Bellas (NASA Ames), Michele Capriati, Olivier Chazot, Anabel del Val (U Minnesota), Bruno Dias (NASA Ames), Giuseppe Gangemi, Bernd Helber, Damien Le Quang, Pietro Parodi, Pierre Schrooyen, JB Scoggins (NASA Langley), Erik Torres (U Minnesota), & Alessandro Turchi (ASI)

- Support from
  - European Research Council (StG #259354 and PoC #713726)
  - FWO and FRIA fellowship program
  - European Space Agency GSTP and TRP programs
  - US Air Force Office of Scientific Research program